On-Surface Synthesis | Very Important Paper

How to cite: *Angew. Chem. Int. Ed.* **2021**, *60*, 25224–25229
International Edition: doi.org/10.1002/anie.202108301
German Edition: doi.org/10.1002/ange.202108301

On-Surface Synthesis and Collective Spin Excitations of a Triangulene-Based Nanostar

Jeremy Hieulle[+], Silvia Castro[+], Niklas Friedrich, Alessio Vegliante, Francisco Romero Lara, Sofía Sanz, Dulce Rey, Martina Corso, Thomas Frederiksen, Jose Ignacio Pascual,* and Diego Peña**

Dedicated to Professor Ben L. Feringa on the occasion of his 70th birthday

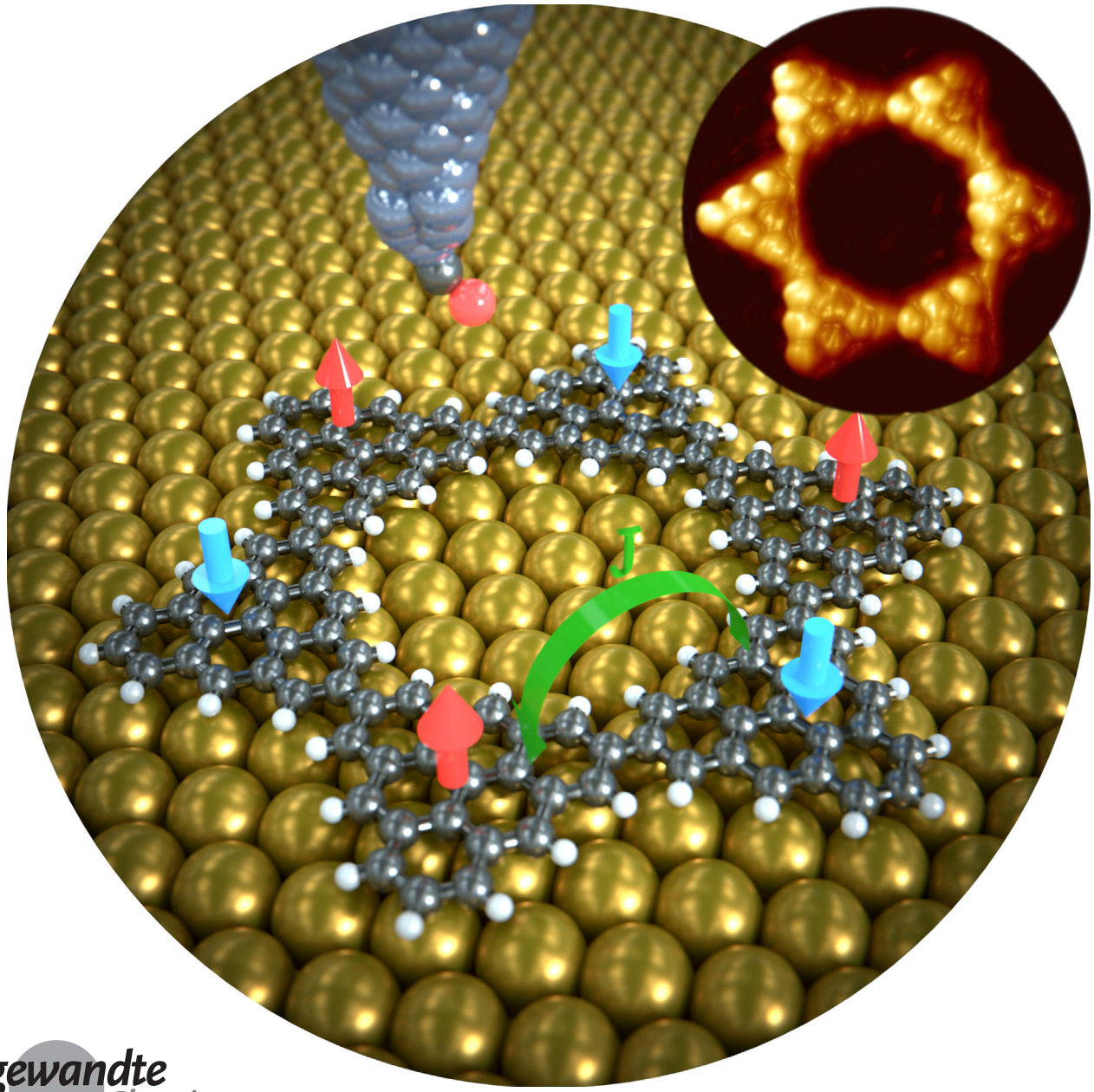

Abstract: *Triangulene nanographenes are open-shell molecules with predicted high spin state due to the frustration of their conjugated network. Their long-sought synthesis became recently possible over a metal surface. Here, we present a macrocycle formed by six [3]triangulenes, which was obtained by combining the solution synthesis of a dimethylphenyl-anthracene cyclic hexamer and the on-surface cyclodehydrogenation of this precursor over a gold substrate. The resulting triangulene nanostar exhibits a collective spin state generated by the interaction of its 12 unpaired π-electrons along the conjugated lattice, corresponding to the antiferromagnetic ordering of six $S=1$ sites (one per triangulene unit). Inelastic electron tunneling spectroscopy resolved three spin excitations connecting the singlet ground state with triplet states. The nanostar behaves close to predictions from the Heisenberg model of an $S=1$ spin ring, representing a unique system to test collective spin modes in cyclic systems.*

Open-shell nanographenes have emerged as privileged testing ground to study carbon-based magnetism and to explore potential applications of organic molecules in spintronics and quantum technologies.[1,2] However, the atomically precise preparation of such nanostructures is challenging due to the high reactivity of these graphene derivatives with radical character under ambient conditions. In this sense, on-surface synthesis under ultra-high vacuum (UHV) has become an interesting alternative to fabricate and study the potential functionality of open-shell carbon nanostructures.[3,4] A paramount example is the preparation of [3]triangulene (Figure 1a), a non-Kekulé triangular-shaped polycyclic aromatic hydrocarbon with two unpaired π electrons, which was finally generated and visualized on a surface by means of scanning probe microscopy (SPM),[5] after previous unsuccessful attempts by solution chemistry methods.[6,7] The particular diradical character of [3]triangulene with $S=1$, makes it a perfect building block for the design of open-shell carbon-based nanostructures with different ground state spin quantum numbers. In fact, during the last three years, the development of triangulene-based nanographenes has been impressive; not only larger triangulenes, such as [4]-, [5]- and [7]-triangulene,[8–10] but other appealing structures such as a [7]triangulene-ring,[11] an extended version of [3]triangulene,[12] or [3]triangulene dimers[13] were prepared by on-surface synthesis. Even the iconic Clar's goblet, which is actually formed by two fused [3]triangulenes sharing one benzene ring, was generated and characterized on-surface.[14] Interestingly, many of these triangulene-based nanostructures exhibit a characteristic low-energy spectral fingerprint associated with spin excitations induced by inelastic tunneling electrons, which was not observed in isolated triangulene units. Such inelastic features provide unique access to quantify spin interactions in nanographenes and to test current theoretical models for describing collective spin states.

In this work, we present a new triangulene derivative consisting in six [3]triangulene moieties arranged in a macrocycle, forming a triangulene-based nanostar (**TNS**) with a pore size of 1.2 nm (Figure 1b). Besides the captivating structure of this carbon-based nanosized molecular star, we were particularly intrigued by the spin configuration adopted by the 12 interacting unpaired electrons in the cyclic hexamer over a metal substrate.

We envisioned the preparation of **TNS** by the on-surface cyclodehydrogenation (CDH) of macrocycle **1** (Figure 1b), in particular by the efficient formation of 12 C–C bonds (in blue) and 12 π radicals in one annealing step promoted by Au(111) under UHV conditions. We selected 2,7-dibromo-10-(2,6-dimethylphenyl)-anthracene (**2**) as triangulene building block with the appropriate bromine disposition for the generation of the cyclic hexamer **1** by surface-assisted Ullmann-coupling. Compound **2** was obtained in one step by reaction of dibromoanthrone **3** with (2,6-dimethylphenyl)-lithium, followed by acid-promoted dehydration (see supporting information (SI) for details). However, in our hands, the on-surface polymerization of compound **2** resulted in a wide variety of triangulene-based oligomers, as it has been independently reported very recently.[15] Therefore, inspired by the synthesis of "*nano-saturns*" by Toyota and co-workers,[16] we decided to attempt the preparation of macrocycle **1** by means of in-solution coupling of dibromoanthracene **2**. In fact, Ni-catalyzed Yamamoto coupling of compound **2** resulted in a mixture of soluble and insoluble oligomers, which, after purification by filtration and washing procedures, led to the isolation of **TNS** precursor **1** in 10% yield.

Despite the large molecular mass of macrocycle **1** ($C_{132}H_{96}$, 1680 Da), its vacuum deposition was possible by

[*] Dr. S. Castro,[+] Dr. D. Rey, Prof. Dr. D. Peña
Centro Singular de Investigación en Química Biolóxica e Materiais Moleculares (CiQUS) and Departamento de Química Orgánica, Universidade de Santiago de Compostela
15782-Santiago de Compostela (Spain)
E-mail: diego.pena@usc.es

Dr. J. Hieulle,[+] N. Friedrich, A. Vegliante, F. R. Lara, Dr. J. I. Pascual
CIC nanoGUNE-BRTA
20018 Donostia-San Sebastián (Spain)
E-mail: ji.pascual@nanogune.eu

F. R. Lara, Dr. M. Corso
Centro de Física de Materiales CSIC/UPV-EHU-Materials Physics Center, 20018 Donostia-San Sebastián (Spain)

S. Sanz, Dr. M. Corso, Dr. T. Frederiksen
Donostia International Physics Center (DIPC)
20018 Donostia-San Sebastián (Spain)
E-mail: thomas_frederiksen@ehu.eus

Dr. T. Frederiksen, Dr. J. I. Pascual
Ikerbasque, Basque Foundation for Science
48013 Bilbao (Spain)

[+] These authors contributed equally to this work.

Supporting information and the ORCID identification number(s) for the author(s) of this article can be found under: https://doi.org/10.1002/anie.202108301.

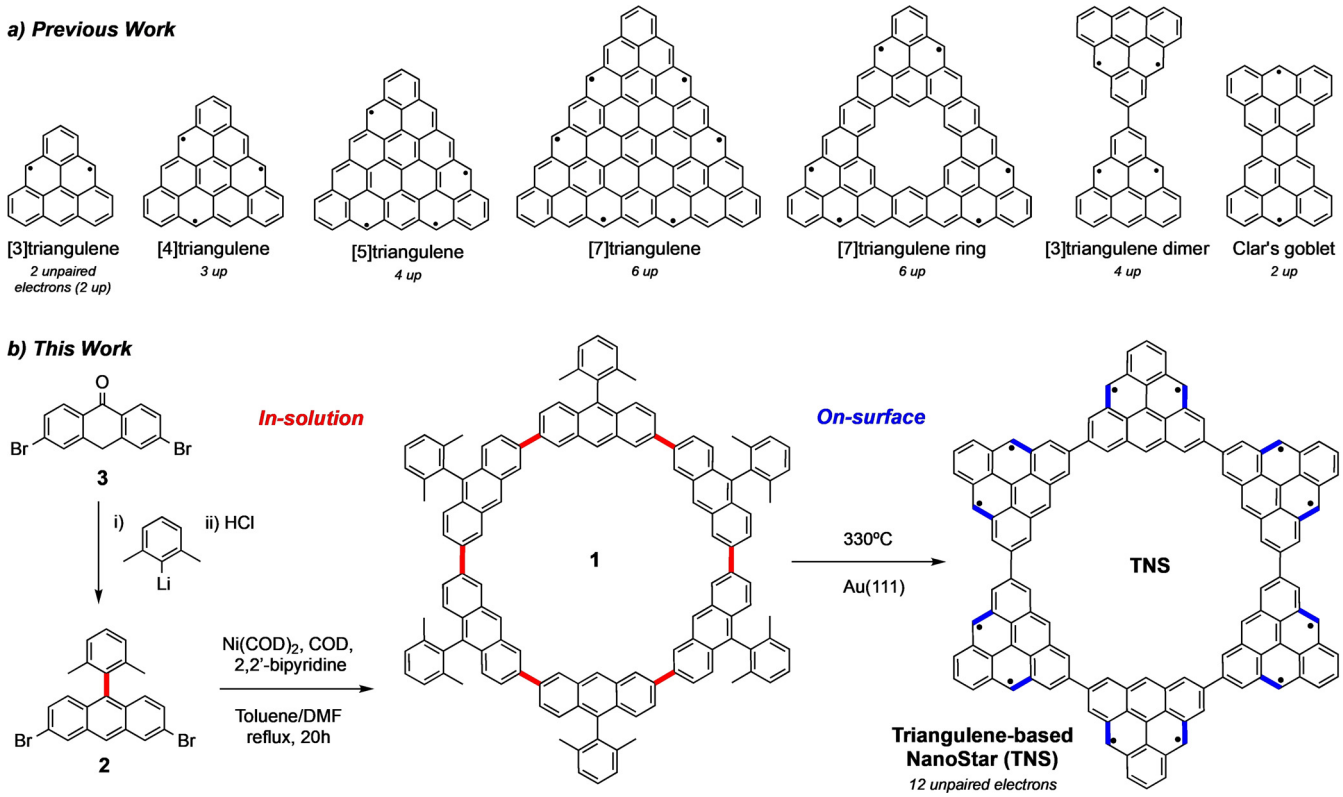

Figure 1. a) Previously reported triangulene derivatives. b) Synthesis of triangulene-based nanostar (**TNS**) developed in this work, by combining in-solution and on-surface chemistry.

flash-annealing a silicon wafer loaded with grains of this compound. Figure 2a shows an overview STM image of the Au(111) substrate after deposition. Molecular rings surviving thermal sublimation appear in closed-packed molecular islands, surrounded by polymeric fragments, probably from rings broken during the thermal sublimation (for the coverage of Figure 2a, about 8% of the material deposited corresponds to intact precursor **1**). Individual molecules **1**, extracted from the domains by lateral manipulation with the STM tip, appear composed of six protrusions corresponding to the six dimethylphenyl groups attached to the anthracenes moieties (Figure 2b).

To induce the full planarization of the macrocycle **1** into the targeted **TNS**, we annealed the substrate to 330 °C. At this temperature, the CDH reaction leading to the formation of π radicals takes place with the removal of 3 H atoms per methyl side group and ring closing through C–C bond formation. However, due to the high temperatures required to fully planarize the whole rings and to their radical character, the CDH competes with additional C–C coupling and bond-breaking reactions, resulting in a few surviving isolated **TNS** (about 20%) and many triangulene oligomers around (Figure 2c and d). Bond-resolved scanning tunneling microscopy (BR-STM) images of molecular rings like in Figure 2d, obtained using a CO functionalized STM tip, resolved the triangulene units connected in a closed ring structure (Figure 2e), in agreement with the expected structure of **TNS** (Figure 1b). The planarization reaction involves the formation of twelve six-membered rings, each one at the position of the methyl groups of precursor **1**. The resulting structure accommodates two unpaired π electrons in each triangulene unit, which are expected to interact throughout the conjugated π-lattice and stabilize a collective spin state.[13]

A first inspection of the magnetic interactions in the ring obtained by mean-field Hubbard (MFH) simulations (Figure 3a, see methods in the SI for details) reveals that intra-triangulene parallel magnetic coupling remains strong in the **TNS**, building a total spin $S=1$ in each triangulene unit, and dominating over a weaker anti-parallel coupling between triangulene sub-units.[17,18] Such interaction pattern is expected to lead to a global spin singlet ground state in the **TNS**. Interestingly, antiferromagnetic (AFM) rings of integer spins have been widely studied for demonstrating the Haldane conjecture,[19,20] stating that the spin excitation spectrum of an infinite Heisenberg $S=1$ AFM chain remains gapped, with an energy value close to 0.4 J (J being the Heisenberg exchange constant). Such a gapped spectrum is an anomalous behavior of integer AFM spin chains, which contrasts with the gapless spin excitation of similar chains made of half-integer spins.[20]

To experimentally determine the spin configuration of the **TNS**, we probed their excitation spectrum by Inelastic Electron Tunneling Spectroscopy (IETS).[21,22] Specifically, we measured differential conductance (dI/dV) vs. bias spectra over the sides of triangulene units of a **TNS** and found bias-symmetric stepped features (Figure 3c), which are a characteristic fingerprint of spin excitation induced by inelastic electron tunneling.[13,14,23] All triangulene units show spectra

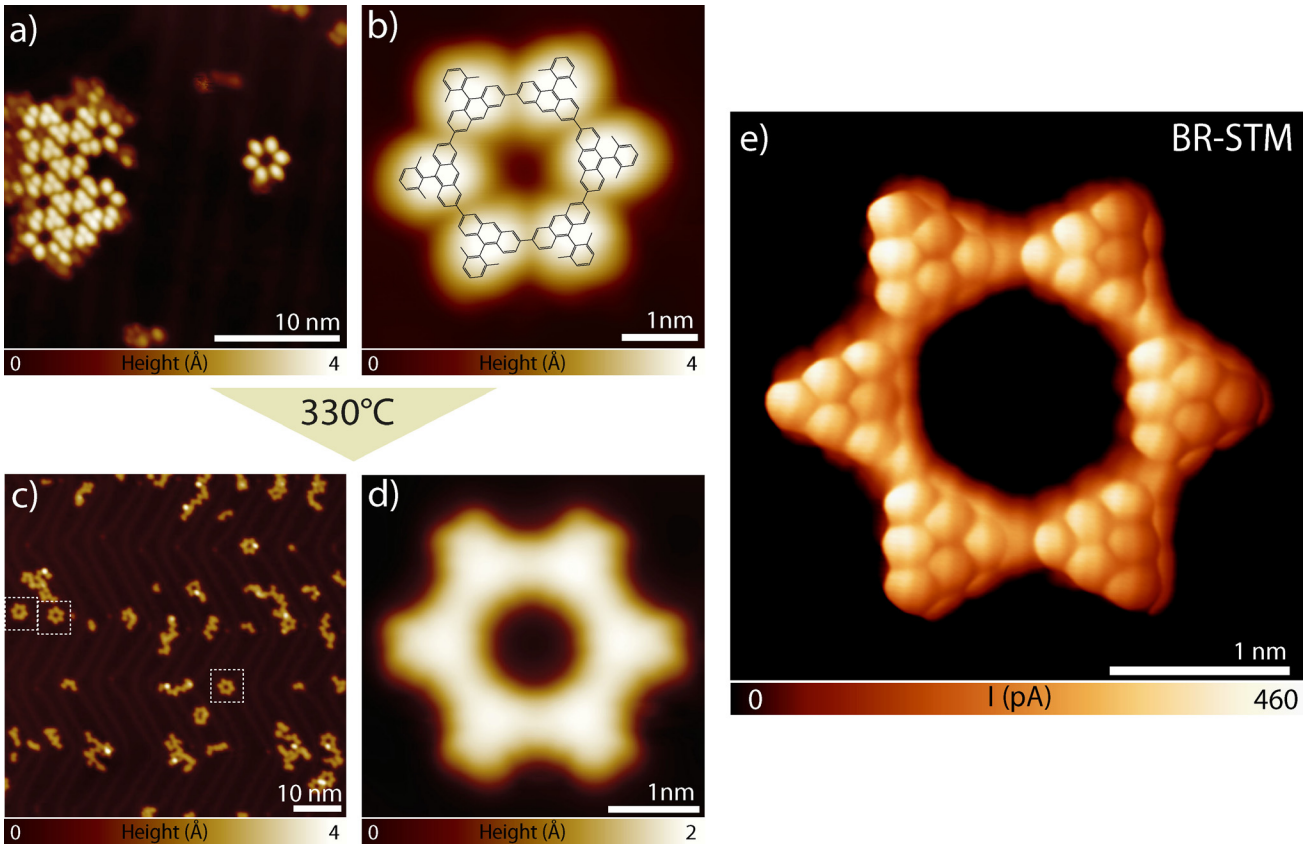

Figure 2. On-surface synthesis of triangulene-based nanostar (**TNS**). a,b) STM images of precursor **1** as deposited on the Au(111) substrate. Molecular rings appear assembled in packed domains. The isolated molecule **1** in (b) was extracted using the STM tip, to prove the covalent nature of the macrocycle. c) STM image of the surface after annealing. **TNS** and fragments appear mostly planarized. d) STM image of a **TNS** formed after thermal annealing. e) BR-STM image of a **TNS**. (a: $V=0.5$ V, $I=60$ pA; b: $V=-0.2$ V, $I=40$ pA; c: $V=1$ V, $I=40$ pA; d: $V=1$ V, $I=100$ pA; e: $V=5$ mV). Data analysis using WSxM.[30]

with the same shape (see additional data in SI), composed of three steps of different height at $E_1=\pm 14(1)$ mV, $E_2=\pm 42(2)$ mV and $E_3=\pm 80(2)$ mV. The first two dI/dV steps have similar height (each amounting to a relative increase of conductance of $\approx 35\,\%$), while the third one appears with small spectral weight ($<7\,\%$). As we show in the stacked dI/dV plot of Figure 3d, the inelastic signal appears localized over the edges of the triangulene units. Such localization pattern is clearly pictured by mapping the inelastic signal d^2I/dV^2 over the whole TNS (shown in SI), confirming that the excitation probability of collective spin states coincides with the larger spin density over edge sites expected for π-radical states.

The presence of three spin excitation steps in the dI/dV spectra is a remarkable feature that contrasts with the single-stepped spectra measured in triangulene dimers[13] and other graphene nanostructures.[14,23–25] Due to the $\Delta S=0,\ \pm 1$ selection rule imposed by conservation of angular momentum,[21] single IETS steps were attributed to singlet-triplet transitions induced by the tunneling electrons. The multi-step spectrum found for the **TNS** unveils a complex excitation pattern of collective spin states in the triangulene ring, accessible by inelastic tunneling electrons.

To unravel the origin of the inelastic steps, we modeled the coupled spin system with an isotropic Heisenberg Hamiltonian describing the AFM exchange interaction of six $S=1$ spins in a closed ring, as in Figure 3e (theoretical details in SI). The many-body ground state of the TNS, obtained by numerically exact diagonalization of the spin Hamiltonian (see methods in SI), has a total spin $S_T=0$ (singlet), and consists of the superposition of the classical solutions of antiferromagnetically coupled triangulene segments (i.e. ground state from the MFH model,[26] in Figure 3a), and other combinations of the triangulene spins with global spin $S_T=0$. Similarly, the set of excited states of the TNS are collective spin modes with total spin amounting from $S_T=0$ to $S_T=6$, which can be described as a superposition of triangulene $S=1$ multiplet states.

To explain the spin excitation spectrum, we assume that steps correspond to transitions with $\Delta S=\pm 1$[27] and adjust the Heisenberg exchange constant J to fit the lowest allowed excitation with the first dI/dV step (centered at ± 14 mV). The best spectral match occurs using $J=18$ meV. This value is larger than the exchange constant derived from the Heisenberg model in triangulene dimers.[13] Figure 3f shows the computed excitations with energy up to 100 meV, classified according to their global spin (up to $S_T=3$). Several singlet and triplet excited states appear within the energy window of the IETS spectrum, including triplet states grouped around excitation energy values (13 meV, 45 meV and 88 meV) that

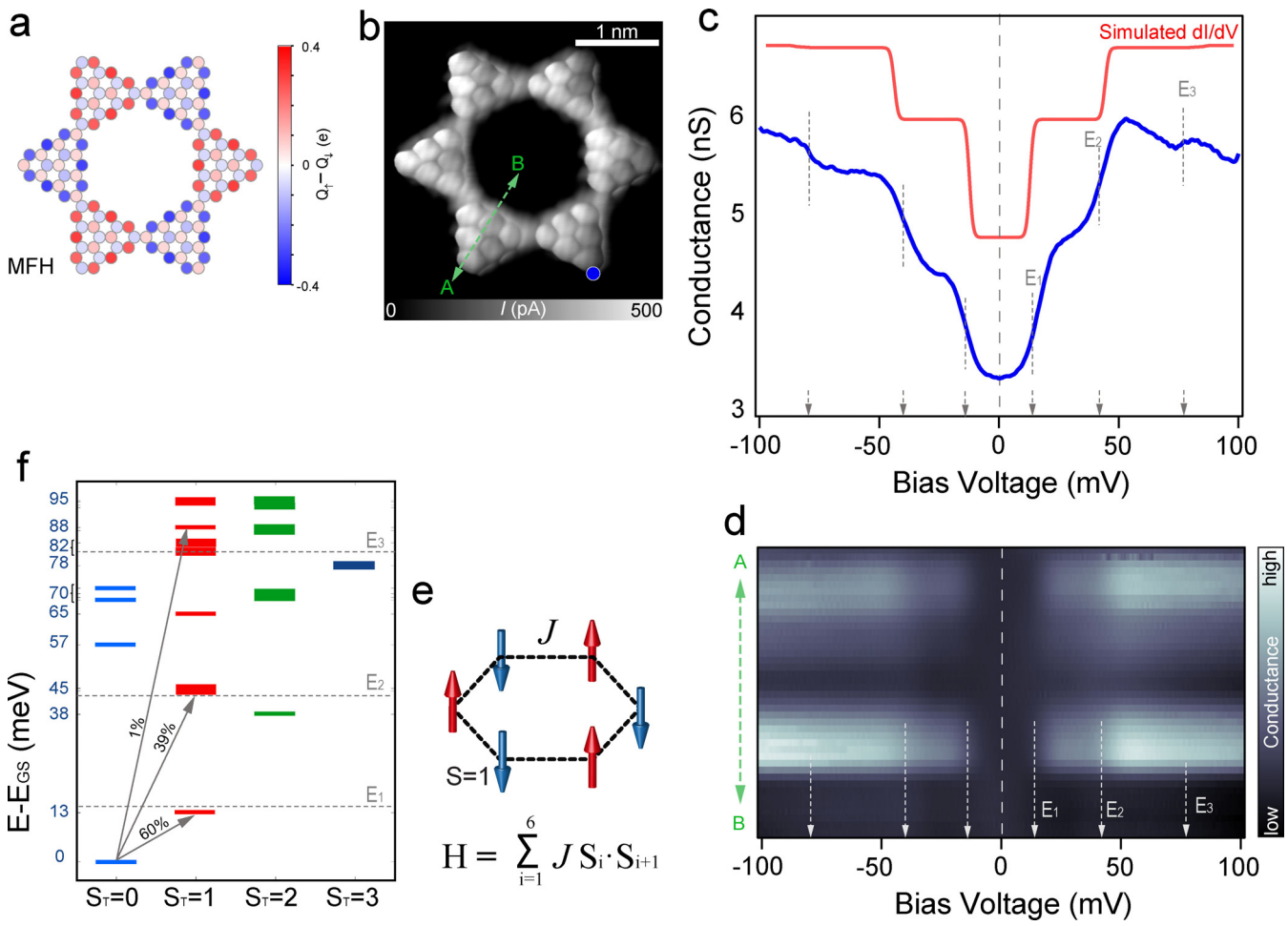

Figure 3. Collective spin excitations in a triangulene-based nanostar. a) Spin density map of a **TNS** obtained from mean-field Hubbard simulations (on-site Coulomb potential $U = 3.5$ eV). b) BR-STM image indicating the **TNS** site where spectra in (c) and line spectra in (d) were taken. c) dI/dV spectrum on a triangulene unit of a **TNS**, showing inelastic steps at $E_1 = \pm 14$ mV, $E_2 = \pm 42$ mV and $E_3 = \pm 80$ mV. The red line shows the simulated spectral function from the Heisenberg model with exchange constant $J = 18$ meV. d) dI/dV spectral line measured across the single triangulene unit indicated in (b). The excitation steps appear around the borders of the **TNS**. Set-point: $V = 100$ mV, $I = 0.1$ nA; individual spectra were offsetted to appear with the same zero-bias conductance. e) Model of a six-membered ring of spin-1, simulated using the Spin Hamiltonian shown in the panel. f) Excitations of the collective spin states obtained from a Heisenberg model with $J = 18$ meV (only states up to $S_T = 3$ are shown). Thin/thick lines indicate singly/doubly degenerate total spin states. Arrows mark the three dominant transitions induced by tunneling electrons (see SI), which coincide in energy and weight with the three steps in the experimental plot in (c).

agree with the three dI/dV steps in our experimental spectra. However, not all transitions are equally accessible by tunneling electrons. To account for the cross-section of each spin transition and explain their different dI/dV step height, we calculated the correlation of collective **TNS** spin states with tunneling electrons following the expression by Ternes.[28] This quantity reflects the scattering probability of a tunnel electron with every collective spin eigenstate and, thus, it is related to the inelastic signal and, hence, to the step height. The first excitation at 13 meV has the larger spectral weight ($\approx 60\,\%$, as shown by arrows in Figure 3 f), while several states bundled at around $E_2 = 45$ meV contribute to most of the remaining weight (39 %). Higher states are seemingly weaker in terms of spectral weight and produce a faint step in the spectrum. A simulated spin excitation spectrum shown in Figure 3 c (red plot) reproduces with good agreement the position and relative intensity of the three steps observed in the experimental plot. There are, however, small differences in step position and height that can be accounted for by including a more precise description of spin interactions. For example, including a finite intra-triangulene coupling can correctly reproduce the equal height of first and second steps (see analysis for twelve 1/2 spins in the SI). Other effects such as a renormalization of spin interactions in the **TNS** induced by the metal substrate,[29] or higher order correction to the Heisenberg coupling between spins,[15,18] can be additionally incorporated into the model to quantitatively reproduce the experimental spectra.

In summary, we have demonstrated the successful fabrication of a macrocycle formed by the covalent attachment of six [3]triangulenes, through a combination of solution synthesis coupling and on-surface planarization. The design-driven strategy of precursor molecules is thus a possible method to produce monodispersed ensembles of complex open-shell nanostructures. For the presented case, the triangulene cyclic hexamer accumulated 12 unpaired electrons.

Tunnel spectroscopy revealed that the unique spin states expected for such interacting systems survive on a metal surface. We detected three collective spin excitations from the many-body singlet ground state to triplet states of the spin ring. These findings proved that the spin states of the nanostar are compatible with an antiferromagnetic $S = 1$ spin ring.

Acknowledgements

We acknowledge funding from Agencia Estatal de Investigación (PID2019-107338RB, FIS2017-83780-P, MDM-2016-0618), from the Xunta de Galicia (Centro singular de investigación de Galicia, accreditation 2019–2022, ED431G 2019/03), the Basque Government (Grant IT1255-19), the European Union H2020 program (FET Open project SPRING #863098), the European Regional Development Fund and the Basque Departamento de Educación for the PhD scholarship no. PRE_2020_2_0049 (S.S.) The authors thank D. Pérez and E. Guitián for fruitful discussions.

Conflict of Interest

The authors declare no conflict of interest.

Keywords: bond-resolved STM · on-surface synthesis · open-shell · spin excitation · triangulene

[1] J. Liu, X. Feng, *Angew. Chem. Int. Ed.* **2020**, *59*, 23386 – 23401; *Angew. Chem.* **2020**, *132*, 23591 – 23607.
[2] W. Zeng, J. Wu, *Chem* **2021**, *7*, 358 – 386.
[3] S. Song, J. Su, M. Telychko, J. Li, G. Li, Y. Li, C. Su, J. Wu, J. Lu, *Chem. Soc. Rev.* **2021**, *50*, 3238 – 3262.
[4] S. Clair, D. G. de Oteyza, *Chem. Rev.* **2019**, *119*, 4717 – 4776.
[5] N. Pavliček, A. Mistry, Z. Majzik, N. Moll, G. Meyer, D. J. Fox, L. Gross, *Nat. Nanotechnol.* **2017**, *12*, 308 – 311.
[6] E. Clar, D. G. Stewart, *J. Am. Chem. Soc.* **1953**, *75*, 2667 – 2672.
[7] G. Allinson, R. J. Bushby, J.-L. Paillaud, *J. Am. Chem. Soc.* **1993**, *115*, 2062 – 2064.
[8] S. Mishra, D. Beyer, K. Eimre, J. Liu, R. Berger, O. Gröning, C. A. Pignedoli, K. Müllen, R. Fasel, X. Feng, P. Ruffieux, *J. Am. Chem. Soc.* **2019**, *141*, 10621 – 10625.
[9] J. Su, M. Telychko, P. Hu, G. Macam, P. Mutombo, H. Zhang, Y. Bao, F. Cheng, Z.-Q. Huang, Z. Qiu, S. J. R. Tan, H. Lin, P. Jelínek, F.-C. Chuang, J. Wu, J. Lu, *Sci. Adv.* **2019**, *5*, eaav7717.
[10] S. Mishra, K. Xu, K. Eimre, H. Komber, J. Ma, C. A. Pignedoli, R. Fasel, X. Feng, P. Ruffieux, *Nanoscale* **2021**, *13*, 1624 – 1628.
[11] J. Su, W. Fan, P. Mutombo, X. Peng, S. Song, M. Ondraćek, P. Golub, J. Brabec, L. Veis, M. Telychko, P. Jelínek, J. Wu, J. Lu, *Nano Lett.* **2021**, *21*, 861 – 867.
[12] J. Li, S. Sanz, J. Castro-Esteban, M. Vilas-Varela, N. Friedrich, T. Frederiksen, D. Peña, J. I. Pascual, *Phys. Rev. Lett.* **2020**, *124*, 177201.
[13] S. Mishra, D. Beyer, K. Eimre, R. Ortiz, J. Fernández-Rossier, R. Berger, O. Gröning, C. A. Pignedoli, R. Fasel, X. Feng, P. Ruffieux, *Angew. Chem. Int. Ed.* **2020**, *59*, 12041 – 12047; *Angew. Chem.* **2020**, *132*, 12139 – 12145.
[14] S. Mishra, D. Beyer, K. Eimre, S. Kezilebieke, R. Berger, O. Gröning, C. A. Pignedoli, K. Müllen, P. Liljeroth, P. Ruffieux, X. Feng, R. Fasel, *Nat. Nanotechnol.* **2020**, *15*, 22 – 28.
[15] S. Mishra, G. Catarina, F. Wu, R. Ortiz, D. Jacob, K. Eimre, J. Ma, C. A. Pignedoli, X. Feng, P. Ruffieux, J. Fernández-Rossier, R. Fasel, *Nature* **2021**, https://doi.org/10.1038/s41586-021-03842-3.
[16] Y. Yamamoto, E. Tsurumaki, K. Wakamatsu, S. Toyota, *Angew. Chem. Int. Ed.* **2018**, *57*, 8199 – 8202; *Angew. Chem.* **2018**, *130*, 8331 – 8334.
[17] W. L. Wang, S. Meng, E. Kaxiras, *Nano Lett.* **2008**, *8*, 241 – 245.
[18] O. V. Yazyev, W. L. Wang, S. Meng, E. Kaxiras, *Nano Lett.* **2008**, *8*, 766.
[19] F. D. M. Haldane, *Phys. Rev. Lett.* **1983**, *50*, 1153 – 1156.
[20] J. P. Renard, L. P. Regnault, M. Verdaguer in *Magnetism: Molecules to Materials I: Models and Experiments* (Eds.: J. S. Miller, M. Drillon), Wiley-VCH, Weinheim, **2003**.
[21] C. F. Hirjibehedin, C. P. Lutz, A. J. Heinrich, *Science* **2006**, *312*, 1021 – 1024.
[22] A. Spinelli, B. Bryant, F. Delgado, J. Fernández-Rossier, A. F. Otte, *Nat. Mater.* **2014**, *13*, 782 – 785.
[23] J. Li, S. Sanz, M. Corso, D. J. Choi, D. Peña, T. Frederiksen, J. I. Pascual, *Nat. Commun.* **2019**, *10*, 200.
[24] A. Sánchez-Grande, J. I. Urgel, L. Veis, S. Edalatmanesh, J. Santos, K. Lauwaet, P. Mutombo, J. M. Gallego, J. Brabec, P. Beran, D. Nachtigallová, R. Miranda, N. Martín, P. Jelínek, D. Écija, *J. Phys. Chem. Lett.* **2021**, *12*, 330 – 336.
[25] S. Mishra, X. Yao, Q. Chen, K. Eimre, O. Gröning, R. Ortiz, M. Di Giovannantonio, J. C. Sancho-García, J. Fernández-Rossier, C. A. Pignedoli, K. Müllen, P. Ruffieux, A. Narita, R. Fasel, *Nat. Chem.* **2021**, *13*, 581 – 586.
[26] https://github.com/dipc-cc/hubbard, https://doi.org/10.5281/zenodo.4748765.
[27] R. Ortiz, J. Fernández-Rossier, *Prog. Surf. Sci.* **2020**, *95*, 100595.
[28] M. Ternes, *New J. Phys.* **2015**, *17*, 063016.
[29] D. Jacob, R. Ortiz, J. Fernández-Rossier, *Phys. Rev. B* **2021**, *104*, 075404.
[30] I. Horcas et al., *Rev. Sci. Inst.* **2007**, *78*, 013705.

Manuscript received: June 22, 2021
Version of record online: October 13, 2021

